Biogeosciences Discuss., 8, 10351–10388, 2011
www.biogeosciences-discuss.net/8/10351/2011/
doi:10.5194/bgd-8-10351-2011

Biogeosciences Discussions

Marine bivalve geochemistry and shell ultrastructure from modern low pH environments

S. Hahn[1], R. Rodolfo-Metalpa[2], E. Griesshaber[3], W. W. Schmahl[3], D. Buhl[1], J. M. Hall-Spencer[2], C. Baggini[2], K. T. Fehr[3], and A. Immenhauser[1]

[1]Institute of Geology, Mineralogy and Geophysics, Ruhr-University Bochum, Universitätsstraße 150, 44801 Bochum, Germany
[2]Marine Institute, Marine Biology and Ecology Research Centre, University of Plymouth, A428, Portland Square, Drake Circus, Plymouth, Devon, PL4 8AA, UK
[3]Department of Earth and Environmental Science, Ludwig Maximilian University, Theresienstraße 41, 80333 Munich, Germany

Received: 20 September 2011 – Accepted: 5 October 2011 – Published: 24 October 2011

Correspondence to: S. Hahn (sabine.hahn@rub.de)

Published by Copernicus Publications on behalf of the European Geosciences Union.

Abstract

Bivalve shells can provide excellent archives of past environmental change but have not been used to interpret ocean acidification events. We investigated carbon, oxygen and trace element records from different shell layers in the mussels *Mytilus galloprovincialis* (from the Mediterranean) and *M. edulis* (from the Wadden Sea) combined with detailed investigations of the shell ultrastructure. Mussels from the harbour of Ischia (Mediterranean, Italy) were transplanted and grown in water with mean pH_T 7.3 and mean pH_T 8.1 near CO_2 vents on the east coast of the island of Ischia. The shells of transplanted mussels were compared with *M. edulis* collected at pH ~ 8.2 from Sylt (German Wadden Sea). Most prominently, the shells recorded the shock of transplantation, both in their shell ultrastructure, textural and geochemical record. Shell calcite, precipitated subsequently under acidified seawater responded to the pH gradient by an in part disturbed ultrastructure. Geochemical data from all test sites show a strong metabolic effect that exceeds the influence of the low-pH environment. These field experiments showed that care is needed when interpreting potential ocean acidification signals because various parameters affect shell chemistry and ultrastructure. Besides metabolic processes, seawater pH, factors such as salinity, water temperature, food availability and population density all affect the biogenic carbonate shell archive.

1 Introduction

Over the last two centuries, human activities have increased the atmospheric CO_2 concentration by about 31 % (Lüthi et al., 2008; Solomon et al., 2009). Approximately one third of the anthropogenic carbon added to the atmosphere is absorbed by the oceans. Uptake of atmospheric CO_2 results in a decrease in ocean water pH, an effect referred to as "ocean acidification" (Caldeira and Wickett, 2003). Since pre-industrial times, ocean pH has dropped by about 0.1 units (Key et al., 2004), a further decrease of 0.4 units is predicted to occur until the end of 2100 (Caldeira and Wickett, 2003).

The decrease in ocean pH is expected to be accompanied by an increase in surface water temperatures (Feely et al., 2004; Caldeira and Wickett, 2005; Balch and Fabry, 2008; Rodolfo-Metalpa et al., 2010). Ocean acidification might directly affect marine calcareous organisms since net calcification rates are affected by decreased calcium carbonate saturation (Fabry et al., 2008; Guinotte and Fabry, 2008) and may lead to a change in the distribution pattern and diversity of carbonate shelled organisms in the oceans (Hall-Spencer et al., 2008).

Many previous studies focus on the response of marine calcified organisms to increased CO_2 levels to predict the impact of ocean acidification (Orr et al., 2005; Davies et al., 2007; Fine and Tchernov, 2007; Hoegh-Guldberg et al., 2007; Carroll et al., 2009; Cigliano et al., 2010; Dias et al., 2010; Gutowska et al., 2010; Rodolfo-Metalpa et al., 2010, 2011). There have also been insights gained from the geological archive to interpret past acidification events (Kump et al., 2009) such as the Paleocene-Eocene Thermal Maximum 55 million years ago (PETM; Zachos et al., 2005; Sluijs et al., 2007; Iglesias-Rodriguez et al., 2008; Gibbs et al., 2010). The PETM was characterized by rapid global warming in the order of 5 to 8 °C (Gibbs et al., 2006) and evidence for a significantly lowered seawater pH has been presented (Gibbs et al., 2006; Mutterlose et al., 2007; Pancost et al., 2007; Handley et al., 2008).

Approaches that study cultured model organisms and those that investigate the geological archive both have merits and problems. Brief monitoring and culturing experiments (several months to few years; Klein et al., 1996a; Berge et al., 2006; Thomsen et al., 2010), provide only limited evidence for longer term adaptational strategies of marine ecosystems. On the other hand studies dealing with geological archives suffer from the lack of biological information and are limited by problems of time control. The majority of geological archive work deals with planktonic organisms from core material in the open ocean (Raffi et al., 2005; Gibbs et al., 2006; Giusberti et al., 2007; Mutterlose et al., 2007; Westerhold et al., 2007). In contrast, studies regarding the impact of past acidification events on fossil coastal neritic settings (Scheibner and Speijer, 2008) are scarce.

One of the most promising archives of past coastal seawater properties are bivalves (Buick and Ivany, 2004; Lopez Correa et al., 2005; Latal et al., 2006; Foster et al., 2009). Bivalves are sessile organisms that over time record environmental changes in their aragonitic and calcitic shells (Witbaard et al., 1994; Vander Putten et al., 2000; Elliot et al., 2003; Immenhauser et al., 2005; Hippler et al., 2009) and their shells hardparts have, under favourable conditions, a high fossilization potential (Elorza and GarciaGarmilla, 1996; Gomez-Alday and Elorza, 2003; Immenhauser et al., 2005). The effect of an increasingly acidified oceanic environment on bivalve metabolism and bioperformance has been investigated in a limited number of studies (Bamber, 1987; Michaelidis et al., 2005; Berge et al., 2006; Gazeau et al., 2007).

Here we use the mussels *M. galloprovincialis* exposed to different pH levels along a natural gradient in CO_2 levels near volcanic vents (pH_T range 6.6–7.1) off Ischia (Italy, Mediterranean Sea) and *M. edulis* collected at pH ~ 8.2 (Blackford and Gilbert, 2007) from List (Wadden Sea). The aim was to calibrate the geochemical and ultrastructural responses of *Mytilus* shells to seawater acidification. We explore and combine the potential of three different proxies within the same carbonate archive: (1) shell isotope and major and trace element geochemistry (2) shell ultra- and microstructure imaging and (3) crystallographic texture analysis. The aims of this work are threefold: to test (1) the potential of bivalve archives as recorders of acidified seawater conditions; to test (2) these archives along real-world seawater pH gradients and to provide (3) a basis for the use of fossil bivalve shells as archives of past acidification events. This work has significance for those concerned in paleo-environmental analysis and carbonate archive research.

2 Materials and methods

2.1 Field study

Our field site was on the east coast of Ischia (40°43.81′ N, 13°57.98′ E) south of Castello Aragonese where shallow water vents acidify the water (Fig. 1). The vents

emit gas composed of 90–95 % CO_2, 3–6 % N_2, 0.6–0.8 % O_2, 0.2–0.8 % CH_4 and 0.08–0.1 % Ar and lacked toxic sulphur compounds (Hall-Spencer et al., 2008). The pH_T range was 6.6 to 8.1 depending on distance from the vents. Seawater carbon (DIC) and oxygen isotope values were 1.4 ‰ and 1.2–1.3 ‰ respectively (Table 1). No differences in seawater isotope ratios were noted between test sites. Several adult *M. galloprovincialis* (>40 mm length) collected from the Ischia port were dislocated to a site with normal pH_T (C in Fig. 1; mean pH_T 8.07) and to a site with acidified seawater (B1 in Fig. 1; mean pH_T 7.25, minimum pH_T 6.83). Samples were labelled with a yellow marker glued onto the shell edge (Fig. 2b) to differentiate between shell precipitated before and after transplantation. The mussels were kept at the test sites for 68 days (28 September to 2 December 2009). Seawater temperature, pH_T and total alkalinity (At) were monitored for the duration of the experiment (Table 1). Oxygen and carbon isotope values of the ambient seawater are from Pierre (1999; Table 1).

Mytilus galloprovincialis lives in intertidal and shallow subtidal waters in temperate estuarine and open coastal settings. This species tolerates a wide range of conditions and is found at salinity from 12 to 38 (Bayne, 1976) and seawater temperatures of 7–27 °C (Aral, 1999). The shells of *M. galloprovincialis* and *M. edulis* are both built from calcite and aragonite and the two species hybridise along the European coast (Daguin et al., 2001; Beaumont et al., 2004).

Mytilus edulis is widespread in shallow temperate and boreal waters (Beesley et al., 2008). Shells of dead *M. edulis* were collected from an intertidal mussel bed near the Island of Sylt (List, Wadden Sea Station). Shells were 1.8–5.5 cm long and the periostracum was abraded or absent. Water temperature at the sampling site was 10–12 °C, pH was around ~8.2 (Blackford and Gilbert, 2007) and the salinity was around 29.5 (28 during winter and 31.6 during summer).

2.2 Materials: structure of mytilid shells

Mussel shells have three layers: the periostracum and two calcium carbonate layers (Figs. 2 and 3). The periostracum forms a quinone-tanned protein layer on the outside

of the shell (Figs. 2a and 3c; Kennedy et al., 1969), the shell, provides a support for calcium carbonate crystals and serves as a seal of the extrapallial space for the achievement of supersaturation conditions (Marin and Luquet, 2004). Carbonate shell layers can be distinguished optically as well as by means of their microstructure and mineralogy. The inner layer consists of iridescent, nacreous aragonite (Fig. 2b; Marin and Luquet, 2004) and is composed of 10–20 µm wide platelets that form parallel arranged 0.5 µm thick laminae (Figs. 2a and 3b). The outer shell layer has a prismatic structure and is composed of calcite fibres (Fig. 3a–d).

2.3 Methods: carbon and oxygen isotope and elemental geochemistry

Carbon and oxygen-isotope analyses of 204 powder samples (170 samples of *M. galloprovincialis* $_{\text{B1 and C}}$ and 34 samples of *M edulis* detailed in Table S3) extracted from mussel shells were performed with a ThermoFinnigan MAT 253 ratio mass spectrometer at the isotope laboratory of the Institute for Geology, Mineralogy and Geophysics (Ruhr-University Bochum, Germany). Repeated analyses of certified carbonate standards (NBS 19, IAEA CO-1 and CO-8) and internal standards show an external reproducibility of ≤ 0.02 ‰ for $\delta^{13}C$ and ≤ 0.06 ‰ for $\delta^{18}O$. All isotope results are reported in per mil (‰) relative to the V-PDB standard in the conventional manner. Two different sampling approaches were applied. One approach used bulk shell samples (including all shell layers and shell layers in variable admixtures; Fig. 2a) following along a transect along the maximum growth axis of the shell. For the second approach shells were cut perpendicularly to the maximum growth axis and calcite samples were extracted using a micro drilling system (MicroMill, Mechantek; Dettman and Lohmann, 1995). For detailed information of the analytical procedure refer to Immenhauser et al. (2005).

Elemental geochemistry analysis was performed on a *M. galloprovincialis* shell from locality B1 (Fig. 1) using a Cameca SX50 electron microprobe at the Department of Earth and Environmental Sciences of the LMU Munich; Germany. The probe was operated at 15 keV acceleration and 20 nA beam current. Barium (Ba), Calcium (Ca), Chlorine (Cl), Iron (Fe), Magnesium (Mg), Manganese (Mn), Phosphorus (P), Silicon

(Si), Sodium (Na) and Strontium (Sr) was measured. Albite (Na), apatite (Ca and P), baryte ($BaSO_4$) (Ba), Fe_2O_3 (Fe), ilmenite ($MnTiO_3$) (Mn), periclase (Mg), $SrSO_4$ (Sr), vanadite (Cl) and wollastonite (Si) were used as standards. Matrix correction was performed by the PAP procedure (Pouchou and Pichoir, 1984). The reproducibility of standard analyses was <1 % for each routinely analysed element. The PAP corrected data were stoichiometrically calculated as carbonate.

Measurements were taken over the entire shell but emphasis was placed on the shell (Fig. 2b) formed directly before and after the transplantation.

2.4 Methods: shell microstructure and texture analysis

The microstructure and texture of *M. galloprovincialis* and *M. edulis* shells were investigated under a scanning electron microscope (SEM) using polished thin sections and fragments of surface samples as well as under electron backscatter diffraction (EBSD). Sections were cut along the median plane of the shells and ~200 µm thick shell wafers were obtained for each investigated specimen. These were subsequently prepared on both sides of the shell as highly polished, 150 µm thin sections. The surface of the thin sections was subsequently etched for 45 s with a suspension of alumina nanoparticles. The samples were then cleaned, dried, and coated with the thinnest possible conducting carbon coating. Scanning electron micrographs and EBSD patterns were obtained on a LEO Gemini 1530 SEM and a JEOL JSM 6500F SEM each equipped with the HKL Technology "Channel 5" EBSD system. Images and EBSD patterns were generated using an accelerating voltage of 20 kV and a beam current of 3.0 nA. The lattice orientation of grains was determined with a spatial resolution of 2–3 µm and an absolute angular resolution of ±0.5 degrees. Electron backscatter diffraction patterns with a mean angular uncertainty of 1 degree and above were discarded.

3 Results

3.1 Macroscopic observations

Macroscopic examination of *M. galloprovincialis* $_{B1}$ samples transplanted to the acidified sites (pH_T 7.25, Fig. 2b) developed characteristic features of the periostracum, the calcitic and the aragonitic shell layers: (1) mussels lacked encrusting or colonizing marine biota (Fig. 2b); (2) near the umbo, the oldest part of the shell, the periostracum was abraded while (3) the nacreous layer lacked its normal lustre and was pitted with small holes (~0.1 mm) and scattered with white spots (Fig. 2b). In contrast, *M. galloprovincialis* $_{C}$ from sea water pH_T 8.07 had shell colonizing marine biota and a lustrous nacre layer. *Mytilus edulis* shells from the Wadden Sea (pH ~ 8.2) had a lustrous nacre layer with commonly white or yellowish coloration.

3.2 Shell ultrastructure, microstructure and texture

Figure 2a displays a sketch of the major structural units of the shell's ultrastructure based on SEM observations of *M. galloprovincialis* $_{B1\ and\ C}$ and *M. edulis*. In the following, differences and similarities of shells that represent the pre-transplantation growth period and the post-transplantation growth period are compared.

The thickness of the calcite and aragonite layers varies significantly over the life time of individual specimen whilst the thickness of the periostracum remains more constant. The calcite shell ranges from 120 to 830 µm and the nacre layer ranges from 5 to 1520 µm in thickness (Supplement; Table S1). The calcite shell layer formed after the transplantation to sites B1 and C has thinned to about 70 % in the case of *M. galloprovincialis* $_{B1}$ and to about 55 % of its former thickness in the case of *M. galloprovincialis* $_{C}$ (Table S1). In *M. galloprovincialis* $_{B1}$ the nacreous shell layer was not formed, while it is present in samples from site C as a 5–10 µm thick layer (Table S1).

Figure 3 depicts comparable portions of an *M. edulis* shell and two investigated *M. galloprovincialis* $_{B1\ and\ C}$ shells formed after the transplantation. The calcite layer of samples from normal seawater pH environments (Site C, pH_T 8.07 and List Wadden

Sea, pH ~ 8.2) is well ordered (Fig. 3a–d), while, in contrast, the calcitic layer of the *M. galloprovincialis* $_{B1}$ specimen from the acidified environment (pH_T of 7.25) is highly unordered. This effect is most pronounced in the portion of the shell formed directly after the transplantation into the acidified environment. With time, the shell structure formed under acidified seawater conditions takes up the formerly structured organization, albeit with localized patches of disordered shell calcite fibers (Fig. 3e and f). The later observation is considered significant.

Electron backscatter diffraction measurements from *M. galloprovincialis* $_{B1}$ are displayed in Figs. 4 and 5. The SEM image in Fig. 5 shows the shell's microstructure across the transition from normal to acidified seawater. Calcite fibres formed prior to the transplantation are aligned in parallel. After the transplantation, a microstructural disarrangement of the shell fabric is observed (Fig. 5b). This feature is perhaps best explained as an adaptation shock of the mussel to the transplantation. After adaptation to the new environment, *M. galloprovincialis* $_{B1}$ precipitates an ordered but thinner calcite shell layer with fibres arranged in parallel (Fig. 3e, f).

The shell texture, specifically the 3-D orientation of calcite fibre c-axes, displays a similar transplantation effect (Fig. 4). A well ordered array of calcite fibre c-axes is precipitated prior to the transplantation (Fig. 5b, c). Unordered fibre c-axes characterize the portion of the shell formed directly after the transplantation (Fig. 5b, d). Electron backscatter diffraction projection patterns in Fig. 5d change to an at least bimodal distribution.

3.3 Shell geochemistry

3.3.1 Elemental abundances

Microprobe analysis results of samples obtained from *M. galloprovincialis* $_{B1}$ are listed in Table S2 (Supplement). Magnesium and sodium abundances are summarized in seven distribution pattern maps shown in Figs. 6 and 7. Clear differences in Ca, Mg, Na and P elemental composition between shell portions representing normal and such

representing acidified seawater are recognized. All other elements were either evenly distributed or below detection limit.

While Ca values are around 390 000 ppm (39 wt %) in all measured maps, *P* shows a highly variable concentration distribution pattern of 1510 (0.151 wt %) to 4680 ppm (0.468 wt %). Both elements, however, are enriched in the calcite layer in comparison to the aragonite layer. Magnesium and sodium show opposing distribution patterns. While magnesium is only present in the calcite layer, sodium is present in both, the calcite and the aragonite layer. In contrast to magnesium, however, sodium is more abundant in the nacre layer (10 600 ppm (1.060 wt %)) compared to the calcite layer (about 4500 ppm (0.450 wt %); Table S2). The sodium content decreases continuously from the shell hinge to the most recent portions of the shell.

Magnesium shows a different distribution pattern with increasing and decreasing trends between shell hinge and commissure. In part this distribution is related to the thickness of the nacre versus the calcite layer with Mg incorporated far more substantially into the calcite layer. Initially, Mg increases in abundance from the shell hinge towards the commissure, this as the nacreous shell layer thins whilst the calcitic layer thickens (Table S2). At the commissural end of the shell (i.e. in the youngest portions of the shell), Mg abundances within the calcite layer first increase and then decrease.

3.3.2 Carbon and oxygen isotope ratios from specific shell layers

In order to assess the relative significance of each individual shell layer (periostracum, calcite layer, nacre/aragonite layer) on bulk $\delta^{13}C$ isotope data and in order to capture the internal variability, sub-samples were drilled from individual layers in selected shells (Fig. 2a). Isotope data are listed in Table S3 (Supplement) and shown in Figs. 8 and 9 and seawater isotope values are shown in Table 1. Due to the complexity of the data set, the main features are summarized.

Bulk carbon isotope values from *M. galloprovincialis* $_{B1}$ shells prior to transplantation range from −1.6 to −0.2 ‰ (standard deviation ($\sigma = 0.02$ ‰). Calcite and aragonite $\delta^{13}C$ ratios scatter between 1.3 and −0.3 ‰ ($\sigma = 0.02$ ‰). Shell material from site B1

(pH_T ‰7.25) has $\delta^{13}C$ values of 2.4 ‰ ($\sigma = 0.02$ ‰) (with periostracum) and around 2.0 ‰ ($\sigma = 0.02$ ‰) (without periostracum), i.e. a difference of less than 0.5 ‰.

Furthermore, *M. galloprovincialis* $_{B1\ and\ C}$ and *M. edulis* $\delta^{13}C_{shell}$ values reveal differences between the three layers (Fig. 8 and Table S3). The heaviest $\delta^{13}C_{shell}$ values were recorded in the nacre-layer. Samples from samples combining periostracum and calcite layer and such from the calcite layer alone are depleted in ^{13}C. Calcite and nacre layers data are intermediate. This pattern is well visible in *M. edulis* but not always detectable in *M. galloprovincialis* from sites B and C.

Oxygen isotope ratios were analyzed from the periostracum, the calcite and the nacre layers as well as bulk samples. Results are shown in Table S3 and summarized in Fig. 8. Bulk $\delta^{18}O$ data from *M. galloprovincialis* $_{B1}$ formed prior to transplantation range from −0.4 to 0.6 ‰ ($\sigma = 0.02$ ‰). Without periostracum material, data range from −0.3 to 0.6 ‰ ($\sigma = 0.02$ ‰). In shell material precipitated under acidified seawater conditions, $\delta^{18}O$ bulk ratios are in the order of 0.8 ‰($\sigma = 0.01$ ‰). Without the periostracum, lower values of 0.6 ‰ ($\sigma = 0.02$ ‰) are found. All of these values are depleted in ^{18}O relative to the $\delta^{18}O_{seawater}$ of 1.2–1.3 ‰.

In shells of *M. galloprovincialis* $_{B1\ and\ C}$ the nacre layer is often isotopically depleted. Another feature is that from the oldest shell portions (hinge) to the youngest shell portions (commissure) the $\delta^{18}O$ values of the layers shift gradually to lower values. This includes samples taken from the periostracum and the calcite layer, samples from the calcite layer alone and samples drilled from the calcite and nacre layer (Fig. 8). In contrast, samples drilled along the transect from within the nacre layer remain rather invariant. The above geochemical patterns are not observed in the reference samples of *M. edulis* from the Wadden Sea.

3.3.3 Isotope time series analysis of calcite shell samples: acidified versus normal seawater environments

In order to capture the geochemical pattern contained in shell material across the transplantation interval, a high resolution isotope record focusing on the calcite layer of *M. galloprovincialis* $_{B1}$ and *M. galloprovincialis* $_{C}$ was performed. The data are listed in Table S3 (Supplement) and results are displayed in Fig. 9. The data set is complex and clearly indicates that fractionation patterns in different shell layers of the same mussel differ considerably. The main features are summarized below.

Calcite layer carbon and oxygen isotope ratios of *M. galloprovincialis* $_{B1}$ prior to transplantation range from −2.4 to −0.6 ‰ ($\delta^{13}C_{shell}$; $\sigma = 0.02$ ‰) and −1.4 to 0.1 ‰ ($\delta^{18}O_{shell}$;$\sigma = 0.03$ ‰). Isotope ratios of shell material precipitated directly after the transplantation, are enriched in ^{13}C and range between 0 and 0.3 ‰ ($\sigma = 0.02$ ‰) and ^{18}O (−0.1 and −0.5 ‰; $\sigma = 0.03$ ‰). In calcite precipitated after the adaptation of the shell to acidified seawater at site B1 (Fig. 1), strongly elevated $\delta^{13}C$ ratios of 1.9 to 2.4 ‰ ($\sigma = 0.02$ ‰) and $\delta^{18}O$ ratios of 0.2 to 0.5 ‰ ($\sigma = 0.03$ ‰) are found. The maximum difference in pre- and post-transplantation $\delta^{13}C_{shell}$ is in the order of 4 ‰ and around 1.9 ‰ for $\delta^{18}O_{shell}$. This difference is considerable. The maximum difference in pre- and post-transplantation bulk $\delta^{13}C_{shell}$ is smaller, i.e. up to 2.5 ‰ and about 1.0 ‰ for $\delta^{18}O_{shell}$.

Carbon and oxygen isotope ratios of *M. galloprovincialis* $_{C}$ prior to transplantation range from −2.2 to −0.9 ‰ ($\delta^{13}C_{shell}$; $\sigma = 0.02$ ‰) and −1.4 to −0.9 ‰ ($\delta^{18}O_{shell}$;$\sigma = 0.03$ ‰). Shell material precipitated after the adaptation to the normal seawater conditions at site C (Fig. 1) ranges between −0.7 to −0.1 ‰ ($\delta^{13}C_{shell}$; $\sigma = 0.02$ ‰) and $\delta^{18}O$ ratios of 0.1 to 0.4 ‰ ($\sigma = 0.03$ ‰). The maximum difference in pre- and post-transplantation $\delta^{18}O_{shell}$ is around 1.8 ‰ (2 ‰ for $\delta^{13}C_{shell}$), i.e. about 50 % of the difference found in shells kept under acidified conditions. For bulk samples, the maximum difference in pre- and post-transplantation $\delta^{13}C_{shell}$ is 1.4 ‰ and around ∼1.6 ‰ for $\delta^{18}O_{shell}$.

4 Interpretation and discussion

4.1 *Mytilus* as an experimental organism

The effects of ocean seawater acidification on the bioperformance of the blue mussel *M. edulis* has previously been the topic of mainly biological research. The *M. edulis* group, involving the three species *M. edulis, M. galloprovincialis* and *M. trossulus* (Koehn, 1991; Aguirre et al., 2006) was investigated for growth patterns (shell length), tissue weight and overall activity and health of these organisms (Bamber, 1987; Berge et al., 2006; Beesley et al., 2008). *Mytilus edulis* has a very wide geographical distribution from the subtropics to the Arctic regions, while *M. trossulus* and *M. galloprovincialis* are more environmentally restricted (Gosling, 2003), but tolerate a wide temperature range (Aral, 1999). The environmental adaptability of *M. edulis* with respect to its wide distribution range including freshwater (Shumway, 1977; Gillikin et al., 2006a, b; Tynan et al., 2006), brackish (Hietanen et al., 1988) and marine settings qualifies the blue mussel as an adaptable and widely used test organism.

All mussels of the *M. edulis* group show a distinct biological control on biomineralization (Heinemann et al., 2008) and, in their rather complex, tripartite shell structure (Fig. 2), a high level of mineralogical and geochemical complexity. The data shown here are clear evidence that this internal complexity is underexplored from the viewpoint of geochemistry and crystallography and represents a significant obstacle for those dealing with the paleo-environmental analysis of fossil material. Particularly, the data shown in Figs. 8 and 9 underscore the notion that different shell layers record environmental parameters in a different manner.

4.2 Sensitivity of *Mytilus* shell geochemistry and ultrastructure to environmental change

Previous studies (Lorens and Bender, 1977; Klein et al., 1996a, b; Vander Putten et al., 2000; Dalbeck et al., 2006; Wanamaker et al., 2007; Heinemann et al., 2008) explore

the impact of seawater salinity and temperature on mainly the carbon and oxygen isotope and elemental signature of *Mytilus* shells, whilst more recent work involves non-traditional isotope systems (Hippler et al., 2009). The geochemical archive of the bivalve shell and here in particular bulk $\delta^{13}C$ and $\delta^{18}O$ isotope analysis provide, if properly interpreted, insight in paleo-environmental parameters. Most researchers agree that for example *Mytilus* shell $\delta^{18}O$ is not influenced by kinetic effects (Klein et al., 1996a), but rather by seawater temperature, salinity and pH a view that is questioned based on the data shown here.

The maximum $\Delta^{18}O_{shell}$ in pre- and post-transplantation is 1.9‰. The shift from lighter to heavier $\delta^{18}O_{shell}$ ratios (Fig. 9b, d), reflects, in the view of the authors, only in part the abrupt transplantation change from warmer harbour temperatures (> 22 °C) to cooler water masses at the test site (20.7 °C; site B1; Fig. 1). None of these abrupt changes in $\delta^{18}O_{shell}$ are observed in the reference mussels from the Wadden Sea (Fig. 9e, f) where the temperature are more stable than the temperate warm Mediterranean. Applying the temperature equation of Anderson and Arthur (1983) for calcite to the *M. galloprovincialis* shell data shown in Fig. 9, a shell $\delta^{18}O$ ratio of −1.5‰ corresponds to a seawater temperature of about 22.5 °C, a value that is in reasonable agreement with average harbour water temperatures. We here propose that transplanted mussels had suffered during the summer 2009, i.e. before the transplantation, from an anomalous warm and long heat-wave, which caused massive mortalities of corals, gorgonians, sponges and bivalves around Ischia (Rodolfo-Metalpa et al., 2011). This heat wave is recorded in the negative shift in shell $\delta^{18}O$ values directly prior to the transplantation (Fig. 9b, d).

Peak oxygen isotope values of 0.5‰, in contrast, measured from shell calcite precipitated after the transplantation to the acidified test site B1 correspond to calculated seawater temperature of 14 °C. This value disagrees with the measured value of about 21 °C (± 4.2 °C) at the test site and indicates that temperature alone, cannot explain the observed pattern. On the level of a working hypothesis, it seems likely, that changes in seawater pH (Bamber, 1987; Michaelidis et al., 2005; Berge et al., 2006; Beesley

et al., 2008) influenced the shell oxygen isotope values, perhaps via calcification rates (Kleypas et al., 1999; Fabry et al., 2008). Seawater pH, however, does not explain the observed isotope shifts in shells dislocated to the experimental site C that is characterized by a normal seawater pH.

Mollusc shell $\delta^{13}C$ has been shown to be related to mainly seasonal changes in food availability (Vander Putten et al., 2000; Wanamaker et al., 2007; Immenhauser et al., 2008). As shown in Fig. 9, $\delta^{13}C$ background ratios of approximately −1 ‰ are found in shell material of *M. galloprovincialis* precipitated prior to transplantation and in such from *M. edulis* from the Wadden Sea. The conspicuously ^{13}C enriched values observed in shells of *M. galloprovincialis* both from experimental site C (pH_T 8.07) and B1 (pH_T 7.25) are probably best understood in the context of sudden, transplantation-related changes in food availability and population density. Remarkably, the $\Delta^{13}C$ from subsamples taken from the shell calcite layer from acidified test site B1 is 4 ‰ (as opposed to 2 ‰ at normal seawater test site C) suggesting an impact of the low seawater pH on either food availability or metabolism.

Shell elemental compositions as shown in Figs. 6 and 7 are difficult to interpret. Obviously, differences in for example Mg abundance between calcite and aragonite are strongly controlled by the crystallographic properties of these carbonate materials. The spatial differences in Ca, Mg, Na and P elemental composition within either aragonite or calcite layers are probably meaningful on the level of biomineralization, i.e. the effect of acidified seawater and other environmental factors on element incorporation. Previous work has documented that Ca^{2+} and Mg^{2+} are transported across the epithelium via inter- and/or intra-cellular pathways (Watabe et al., 1990). Cations are either actively pumped across the cell membrane or move by passive diffusion through extracellular fluids to the site of calcification (Weiner and Dove, 2003; Addadi et al., 2006). At present, the authors accept that a detailed level of knowledge regarding the biologically controlled incorporation of elements in the shell of *M. galloprovincialis* is not reached and an in-depth interpretation of these data is beyond the scope of this paper.

The observed differences in the shell ultrastructure in specimen dislocated to test sites B1 and C are significant and document the sensitivity of this previously underexplored proxy to environmental change. While the portions of the shell, that were biomineralized under normal seawater pH_T of 8.07 (test site C in Fig. 3) are well ordered, the shell portions that precipitated under acidified seawater conditions (site B1; Fig. 1) directly after the transplantation show a highly unstructured shell microstructure. Shell portions precipitated some weeks after the transplantation are rather well structured but contain spatially irregular shell portions with disordered calcite fibres (Fig. 3e, f). These detailed insights into the shell ultrastructure are equally encouraging and illustrated through the measured EBSD maps (Fig. 4).

Another important macroscopic feature refers to the aragonite or nacre layer. In shell material from the acidified test environment B1, the aragonite layer is characterized by small, spatially isolated holes (diameters of ∼0.1 mm), an overall reduced thickness and a dull surface (Fig. 2b). These dissolution effects may be caused by the acid base balance regulation of the mussel in acidified conditions (Michaelidis et al., 2005). Mussels that were transported to site C (pH_T 8.07) lack these features but are in contrast characterized by a highly lustrous nacre layer.

Mytilus galloprovincialis $_{B1\ and\ C}$ show both a distinct thinning of the calcite shell layer directly after the transplantation. A connection with the implementation process itself can not be excluded but the shells remain relatively thin after their adaptation to the new environment. Many independent factors, however, influence bivalve shell formation and thickness. Given that a shell thinning is present at sites with acidified and at sites with normal seawater pH, the relation between shell thickness and environmental factors is probably complex. All of these above features, structured versus unstructured shell organization, differences in the appearance of the nacre layer, calcite layer thinning and marked changes in geochemical signature, have a considerable fossilization potential. These results are considered encouraging.

4.3 Environmental impact versus experimental bias

Mytilus shells are complex biomineral structures (Lowenstam and Weiner, 1989) precipitated under controlled extracellular processes (Crenshaw, 1980; Falini et al., 1996; Gotliv et al., 2003; Gaspard et al., 2008). Factors that affect the complex metabolic processes that in turn govern biomineralization include: (1) environment (Vander Putten et al., 2000) and here particularly seawater temperature (Bauwens et al., 2010), salinity (Bayne, 1976), and pH (Bamber, 1987; Michaelidis et al., 2005; Berge et al., 2006; Beesley et al., 2008); (2) food availability (Gosling, 2003); and (3) the degree of competition and population density (Gosling, 2003). This complicates the interpretation of geochemical and ultrastructural observations shown here. This is because specimen of *M. galloprovincialis* were dislocated to environments not only characterized by different seawater temperatures and pH (Table 1) but where also exposed to sites with, in respect to their former harbour environment, different nutrient levels and test mussels experienced an abrupt change in population density.

In addition to this, specimens were artificially exposed to an abrupt transplantation shock when exposing these mussels to test sites B1 and C. The abrupt change in the spatial orientation of calcite fibres c-axes across the transplantation suture shown in Fig. 5 is perhaps best explained by the transplantation shock because this suture line is present in samples dislocated to acidified seawater site B1 as well as in such brought to normal pH site C. The transplantation shock therefore resulted in artefact features that are not expected in natural settings where environmental changes tend to be more gradual. This includes for example seasonal changes in seawater temperature, food availability but also gradual changes in population density.

The above consideration document the potential limitations of the field experimental setup applied here. First, our experiment was too short (68 days) to allow specimens to recover from the transplantation shock and to fully adapt to normal grow rates. Second, natural settings are by definition complex multi-component systems. This complexity, combined with experimental artefacts such as transplantation shock features limits the

interpretation of geochemical and structural features observed to some degree. Culturing experiments, performed under constant environmental parameters food availability (Thomsen and Melzner, 2010; Thomsen et al., 2010; Heinemann et al., 2011) are poor analogues of naturally complex environments but allow for a precise relation of specific environmental factors to textural or geochemical features observed in the test shells. In this sense, the experiment shown here is considered a successful failure. Successful, as the data shown here clearly document the potential of combined geochemical and shell ultrastructure proxy analysis. A failure, as it is at present not possible to precisely allocate specific environmental parameters to specific geochemical or structural features.

5 Conclusions

Based on the data shown here, the following conclusions are drawn:

1. Live specimen of *M. galloprovincialis* were transplanted from Ischia harbour to nearby CO_2 vents and exposed to mean seawater pH_T 8.07 and 7.25. The shells responded with differential changes in shell carbon, oxygen and elemental composition, by a marked thinning of the calcite layer and by an – at least partial – lack of structure in the orientation of calcite fibres. In addition, the nacreous layer of mussels grown in acidified seawater was thin, dull and had started to dissolve. Test specimen of *M. edulis* from pH 8.2 sites in the Wadden Sea showed none of these features.

2. The marked trends in $\delta^{18}O$ across mussel shells grown after transplantation cannot be explained by seawater temperatures and pH differences alone. Oxygen-based seawater temperature calculations (>14 °C) do not match the measured seawater temperatures of approximately 21 °C. Pending more data, we suspect that mussel metabolism influenced the shell $\delta^{18}O$ ratios.

3. Pronounced shifts in $\delta^{13}C$ may reflect abrupt changes in food availability and population density when the mussels were transplanted to the CO_2 vent area. Remarkably, the $\delta^{13}C$ in the calcite layer of the shells exposed to acidified seawater was about 200 % of that in shells precipitated under normal seawater pH. This point to an influence of seawater pH on bivalve metabolism and probably food availability that is again influenced by seawater pH.

4. Different shell layers, i.e. periostracum, aragonite and calcite layers show remarkable differences in both carbon and oxygen isotope values. This notion questions the value of bulk data from bivalve shells.

5. Differences in shell elemental abundances in mussels exposed to acidified seawater at test sites compared to normal conditions are difficult to interpret. First order elemental differences are related to crystallographical differences between calcite and aragonite. Nevertheless, the spatial differences in Ca, Mg, Na and P elemental composition within one shell layer are highly complex and probably meaningful on the level of metabolic controls during biomineralization.

6. We have documented the successful application of a combined geochemical and shell ultrastructural/textural proxy analysis from complex natural archives. The transplantation shock clearly recorded in the mussel shells is a problem and suggests that specimen must be kept several months at test sites before they adapt to the new environment. Our field experiments show that caution is required when using bivalve shells to interpret past ocean acidification evens as shells can respond to a range of factors along with the effects of high CO_2.

7. It is proposed that the combination of field experiments and laboratory cultures will lead to an improved understanding of factors affecting shell growth and its use in interpretations of ocean acidification events.

Supplementary material related to this article is available online at: http://www.biogeosciences-discuss.net/8/10351/2011/ bgd-8-10351-2011-supplement.pdf.

Acknowledgements. This is a contribution to BioAcid. Kristina Stemmer is acknowledged for providing shells of *M. edulis* and supporting information. We wish to thank Mrs. Enders (LMU Munich) and the laboratory staff at the Ruhr University for analytical support. The project has been supported by FP7 EU MedSeA (265103) and EU MARES. We thankfully acknowledge the support of Federal Ministry of Education and Research (BMBF; FKZ 03F0608H).

References

Addadi, L., Joester, D., Nudelman, F., and Weiner, S.: Mollusk shell formation: A source of new concepts for understanding biomineralization processes, Chemistry, 12, 980–987, 2006.

Aguirre, M. L., Perez, S. I., and Sirch, Y. N.: Morphological variability of brachidontes swainson (bivalvia, mytilidae) in the marine quaternary of Argentina (SW Atlantic), Palaeogr. Palaeocl., 239, 100–125, doi:10.1016/j.palaeo.2006.01.019, 2006.

Anderson, T. F. and Arthur, M. A.: Stable isotopes of oxygen and carbon and their application to sedimentologic and paleoenvironmental problems, Society of Sedimentary Geology, 10, 151, 1983.

Aral, O.: Growth of the mediterranean mussel (*Mytilus galloprovincialis* lam., 1819) on ropers in the black sea, turkey, Turkish Journal of Veterinary & Animal Sciences, 23, 183–189, 1999.

Balch, W. M. and Fabry, V. J.: Ocean acidification: Documenting its impact on calcifying phytoplankton at basin scales, Mar. Ecol.-Pro. Ser., 373, 239–247, doi:10.3354/meps07801, 2008.

Bamber, R. N.: The effects of acidic sea-water on young carpet-shell clams *venerupis-decussata* (l) (mollusca, veneracea), J. Exp. Mar. Biol. Ecol., 108, 241–260, 1987.

Bauwens, M., Ohlsson, H., Barbé, K., Beelaerts, V., Schoukens, J., and Dehairs, F.: A nonlinear multi-proxy model based on manifold learning to reconstruct water temperature from high

resolution trace element profiles in biogenic carbonates, Geosci. Model Dev., 3, 653–667, doi:10.5194/gmd-3-653-2010, 2010.
Bayne, B. L.: Marine mussels, their ecology and physiology, in, Cambridge University Press, Cambridge, UK, 523, 1976.
Beaumont, A. R., Turner, G., Wood, A. R., and Skibinski, D. O. F.: Hybridisations between *Mytilus edulis* and *Mytilus galloprovincialis* and performance of pure species and hybrid veliger larvae at different temperatures, J. Exp. Mar. Biol. Ecol., 302, 177–188, doi:10.1016/j.jembe.2003.10.009, 2004.
Beesley, A., Lowe, D. M., Pascoe, C. K., and Widdicombe, S.: Effects of CO_2-induced seawater acidification on the health of *Mytilus edulis*, Clim. Res., 37, 215–225, doi:10.3354/cr00765, 2008.
Berge, J. A., Bjerkeng, B., Pettersen, O., Schaanning, M. T., and Oxnevad, S.: Effects of increased sea water concentrations of CO_2 on growth of the bivalve *Mytilus edulis* l, Chemosphere, 62, 681–687, doi:10.1016/j.chemosphere.2005.04.111, 2006.
Blackford, J. C. and Gilbert, F. J.: Ph variability and CO_2 induced acidification in the north sea, J. Ma. Sys., 64, 229–241, doi:doi:10.1016/j.jmarsys.2006.03.016, 2007.
Buick, D. P. and Ivany, L. C.: 100 years in the dark: Extreme longevity of Eocene bivalves from Antarctica, Geology, 32, 921–924, doi:10.1130/g20796.1, 2004.
Caldeira, K. and Wickett, M. E.: Anthropogenic carbon and ocean ph, Nature, 425, 365–365, doi:10.1038/425365a, 2003.
Caldeira, K. and Wickett, M. E.: Ocean model predictions of chemistry changes from carbon dioxide emissions to the atmosphere and ocean, J. Geophys. Res.-Oceans, 110, 1–12, doi:10.1029/2004jc002671, 2005.
Carroll, M. L., Johnson, B. J., Henkes, G. A., McMahon, K. W., Voronkov, A., Ambrose, W. G., and Denisenko, S. G.: Bivalves as indicators of environmental variation and potential anthropogenic impacts in the southern Barents Sea, Mar. Poll. Bull., 59, 193–206, doi:10.1016/j.marpolbul.2009.02.022, 2009.
Cigliano, M., Gambi, M. C., Rodolfo-Metalpa, R., Patti, F. P., and Hall-Spencer, J. M.: Effects of ocean acidification on invertebrate settlement at volcanic CO_2 vents, Mar. Biol. (Berlin), 157, 2489–2502, doi:10.1007/s00227-010-1513-6, 2010.
Crenshaw, M. A.: Mechanisms of shell formation and dissolution, in: Skeletal growth of aquatic organisms, edited by: Rhods, D. C., and Lutz, R. A., Plenum Publishing Corporation, New York, 115–132, 1980.

Daguin, C., Bonhomme, F., and Borsa, P.: The zone of sympatry and hybridization of *Mytilus edulis* and *M. galloprovincialis*, as described by intron length polymorphism at locus mac-1, Heredity, 86, 342–354, doi:10.1046/j.1365-2540.2001.00832.x, 2001.
Dalbeck, P., England, J., Cusack, M., Lee, M. R., and Fallick, A. E.: Crystallography and chemistry of the calcium carbonate polymorph switch in *M. edulis* shells, Eur. J. Mineral., 18, 601–609, doi:10.1127/0935-1221/2006/0018-0601, 2006.
Davies, A. J., Roberts, J. M., and Hall-Spencer, J.: Preserving deep-sea natural heritage: Emerging issues in offshore conservation and management, Biol. Conserv., 138, 299–312, doi:10.1016/j.biocon.2007.05.011, 2007.
Dettman, D. L. and Lohmann, K. C.: Microsampling carbonates for stable isotope and minor element analysis – physical separation of samples on a 20 µm scale, J. Sedimen. R. A., 65, 566–569, 1995.
Dias, B. B., Hart, B., Smart, C. W., and Hall-Spencer, J. M.: Modern seawater acidification: The response of foraminifera to high-CO_2 conditions in the Mediterranean sea, J. Geol. Soc., 167, 843–846, doi:10.1144/0016-76492010-050, 2010.
Elliot, M., deMenocal, P. B., Linsley, B. K., and Howe, S. S.: Environmental controls on the stable isotopic composition of *Mercenaria mercenaria*: Potential application to paleoenvironmental studies, Geochem. Geophy. Geosy., 4, 1–16, doi:10.1029/2002gc000425, 2003.
Elorza, J. and GarciaGarmilla, F.: Petrological and geochemical evidence for diagenesis of inoceramid bivalve shells in the plentzia formation (Upper Cretaceous, Basque-Cantabrian region, northern Spain), Cretaceous Res., 17, 479–503, 1996.
Fabry, V. J., Seibel, B. A., Feely, R. A., and Orr, J. C.: Impacts of ocean acidification on marine fauna and ecosystem processes, Ices J. Mar. Sci., 65, 414–432, doi:10.1093/icesjms/fsn048, 2008.
Falini, G., Albeck, S., Weiner, S., and Addadi, L.: Control of aragonite or calcite polymorphism by mollusk shell macromolecules, Science, 271, 67–69, 1996.
Feely, R. A., Sabine, C. L., Lee, K., Berelson, W., Kleypas, J., Fabry, V. J., and Millero, F. J.: Impact of anthropogenic CO_2 on the $CaCO_3$ system in the oceans, Science, 305, 362–366, 2004.
Fine, M. and Tchernov, D.: Ocean acidification and scleractinian corals, Science, 317, 1032–1033, 2007.
Foster, L. C., Allison, N., Finch, A. A., Andersson, C., and Ninnemann, U. S.: Controls on delta $\delta^{18}O$ and delta $\delta^{13}C$ profiles within the aragonite bivalve *Arctica islandica*, Holocene, 19,

549–558, doi:10.1177/0959683609104028, 2009.
Gaspard, D., Marin, F., Guichard, N., Morel, S., Alcaraz, G., and Luquet, G.: Shell matrices of recent rhynchonelliform brachiopods: Microstructures and glycosylation studies, Earth Env. Sci. T. R. So., 98, 415–424, doi:10.1017/s1755691007078401, 2008.
Gazeau, F., Quiblier, C., Jansen, J. M., Gattuso, J. P., Middelburg, J. J., and Heip, C. H. R.: Impact of elevated CO_2 on shellfish calcification, Geophys. Res. Lett., 34, 1–5, doi:10.1029/2006GL028554, 2007.
Gibbs, S. J., Bown, P. R., Sessa, J. A., Bralower, T. J., and Wilson, P. A.: Nannoplankton extinction and origination across the Paleocene-Eocene Thermal Maximum, Science, 314, 1770–1773, doi:10.1126/science.1133902, 2006.
Gibbs, S. J., Stoll, H. M., Bown, P. R., and Bralower, T. J.: Ocean acidification and surface water carbonate production across the Paleocene-Eocene Thermal Maximum, Earth Planet Sci. Lett., 295, 583–592, doi:10.1016/j.epsl.2010.04.044, 2010.
Gillikin, D. P., Dehairs, F., Lorrain, A., Steenmans, D., Baeyens, W., and Andre, L.: Barium uptake into the shells of the common mussel (*Mytilus edulis*) and the potential for estuarine paleo-chemistry reconstruction, Geochim. Cosmochim. Acta, 70, 395–407, doi:10.1016/j.gca.2005.09.015, 2006a.
Gillikin, D. P., Lorrain, A., Bouillon, S., Willenz, P., and Dehairs, F.: Stable carbon isotopic composition of *Mytilus edulis* shells: Relation to metabolism, salinity, delta C-13(dic) and phytoplankton, Org. Geochem., 37, 1371–1382, doi:10.1016/j.orggeochem.2006.03.008, 2006b.
Giusberti, L., Rio, D., Agnini, C., Backman, J., Fornaciari, E., Tateo, F., and Oddone, M.: Mode and tempo of the Paleocene-Eocene Thermal Maximum in an expanded section from the venetian pre-alps, Geol. Soc. Am. Bull., 119, 391–412, doi:10.1130/b25994.1, 2007.
Gomez-Alday, J. J. and Elorza, J.: Diagenesis, regular growth and records of seasonality in inoceramid bivalve shells from mid-maastrichtian hemipelagic beds of the bay of biscay, Neth. J.Geosci., 82, 289–301, 2003.
Gosling, E.: Bivalve molluscs – biology, ecology and culture, in: Fishing news books, Blackwell Publishers, 456, 2003.
Gotliv, B. A., Addadi, L., and Weiner, S.: Mollusk shell acidic proteins: In search of individual functions, Chembiochem, 4, 522–529, doi:10.1002/cbic.200200548, 2003.
Guinotte, J. M. and Fabry, V. J.: Ocean acidification and its potential effects on marine ecosystems, Ann. NY Acad. Sci., 2008, 1134, 320–342, doi:10.1196/annals.1439.013, 2008.
Gutowska, M. A., Melzner, F., Portner, H. O., and Meier, S.: Cuttlebone calcification increases

during exposure to elevated seawater pCO(2) in the cephalopod *Sepia officinalis*, Mar. Biol., 157, 1653–1663, doi:10.1007/s00227-010-1438-0, 2010.
Hall-Spencer, J. M., Rodolfo-Metalpa, R., Martin, S., Ransome, E., Fine, M., Turner, S. M., Rowley, S. J., Tedesco, D., and Buia, M. C.: Volcanic carbon dioxide vents show ecosystem effects of ocean acidification, Nature, 454, 96–99, doi:10.1038/nature07051, 2008.
Handley, L., Pearson, P. N., McMillan, I. K., and Pancost, R. D.: Large terrestrial and marine carbon and hydrogen isotope excursions in a new Paleocene/Eocene boundary section from Tanzania, Earth Planet. Sci. Lett., 275, 17–25, doi:10.1016/j.epsl.2008.07.030, 2008.
Heinemann, A., Fietzke, J., Eisenhauer, A., and Zumholz, K.: Modification of Ca isotope and trace metal composition of the major matrices involved in shell formation of *Mytilus edulis*, Geochem. Geophys., 9, 1–8, doi:10.1029/2007gc001777, 2008.
Heinemann, A., Hiebenthal, C., Fietzke, J., Eisenhauer, A., and Wahl, M.: Disentangling the biological and environmental control of *M. edulis* shell chemistry, Geochem. Geophys., 12, Q05012, doi:10.1029/2011GC003673, 2011.
Hietanen, B., Sunila, I., and Kristoffersson, R.: Toxic effects of zinc on the common mussel *Mytilus edulis* l. (bivalvia) in brackish water, Part 1, Physiological and histopathological studies, Ann. Zool. Fenn., 25, 341–347, 1988.
Hippler, D., Buhl, D., Witbaard, R., Richter, D. K., and Immenhauser, A.: Towards a better understanding of magnesium-isotope ratios from marine skeletal carbonates, Geochim. Cosmochim. Acta, 73, 6134–6146, 2009.
Hoegh-Guldberg, O., Mumby, P. J., Hooten, A. J., Steneck, R. S., Greenfield, P., Gomez, E., Harvell, C. D., Sale, P. F., Edwards, A. J., Caldeira, K., Knowlton, N., Eakin, C. M., Iglesias-Prieto, R., Muthiga, N., Bradbury, R. H., Dubi, A., and Hatziolos, M. E.: Coral reefs under rapid climate change and ocean acidification, Science, 318, 1737–1742, doi:10.1126/science.1152509, 2007.
Iglesias-Rodriguez, M. D., Halloran, P. R., Rickaby, R. E. M., Hall, I. R., Colmenero-Hidalgo, E., Gittins, J. R., Green, D. R. H., Tyrrell, T., Gibbs, S. J., von Dassow, P., Rehm, E., Armbrust, E. V., and Boessenkool, K. P.: Phytoplankton calcification in a high-CO_2 world, Science, 320, 336–340, doi:10.1126/science.1154122, 2008.
Immenhauser, A., Nägler, T. F., Steuber, T., and Hippler, D.: A critical assessment of mollusk O-18/O-16, Mg/Ca, and Ca-44/Ca-40 ratios as proxies for cretaceous seawater temperature seasonality, Palaeogeogr. Palaeocl., 215, 221–237, doi:10.1016/j.palaeo.2004.09.005, 2005.

Immenhauser, A., Holmden, C., and Patterson, W. P.: Interpreting the carbon-isotope record of ancient shallow epeiric seas: Lessons from the recent, in: Dynamics of epeiric seas, edited by: Pratt, B. R., and Holmden, C., Geological Association of Canada Special Publication, 135–174, 2008.
Kennedy, W. J., Taylor, J. D., and Hall, A.: Environmental and biological controls on bivalve shell mineralogy, Biological Review of the Cambridge Philosophical Society, 44, 499–530, 1969.
Key, R. M., Kozyr, A., Sabine, C. L., Lee, K., Wanninkhof, R., Bullister, J. L., Feely, R. A., Millero, F. J., Mordy, C., and Peng, T. H.: A global ocean carbon climatology: Results from global data analysis project (glodap), Global Biogeochem. Cy., 18, GB4031, doi:10.1029/2004gb002247, 2004.
Klein, R. T., Lohmann, K. C., and Thayer, C. W.: Sr/Ca and C-13/C-12 ratios in skeletal calcite of *Mytilus trossulus*: Covariation with metabolic rate, salinity, and carbon isotopic composition of seawater, Geochim. Cosmochim. Acta, 60, 4207–4221, doi:10.1016/S0016-7037(96)00232-3, 1996a.
Klein, R. T., Lohmann, K. C., and Thayer, C. W.: Bivalve skeletons record sea-surface temperature and delta O-18 via Mg/Ca and O-18/O-16 ratios, Geology, 24, 415–418, 1996b.
Kleypas, J. A., Buddemeier, R. W., Archer, D., Gattuso, J. P., Langdon, C., and Opdyke, B. N.: Geochemical consequences of increased atmospheric carbon dioxide on coral reefs, Science, 284, 118–120, 1999.
Koehn, R. K.: The genetics and taxonomy of species in the genus mytilus, Aquaculture, 94, 125–145, 1991.
Kump, L. R., Bralower, T. J., and Ridgwell, A.: Ocean acidification in deep time, Oceanography, 22, 94–107, 2009.
Latal, C., Piller, W. E., and Harzhauser, M.: Shifts in oxygen and carbon isotope signals in marine molluscs from the central paratethys (Europe) around the lower/middle Miocene transition, Palaeogeogr. Palaeocl., 231, 347–360, doi:10.1016/j.palaeo.2005.08.008, 2006.
Lopez Correa, M., Freiwald, A., Hall-Spencer, J., Taviani, M., and Roberts, J. M.: Distribution and habitats of *Acesta excavata* (bivalvia: Limidae) with new data on its shell ultrastructure, Cold-water corals and ecosystems, Erlangen Earth Conf., 173–205, doi:10.1007/3-540-27673-4_9, 2005.
Lorens, R. B. and Bender, M. L.: Physiological exclusion of magnesium from *Mytilus edulis* calcite, Nature, 269, 793–794, 1977.
Lowenstam, H. A. and Weiner, S.: On biomineralization, in, Oxford University Press, Inc., New

York, 324, 1989.
Lüthi, D., Le Floch, M., Bereiter, B., Blunier, T., Barnola, J. M., Siegenthaler, U., Raynaud, D., Jouzel, J., Fischer, H., Kawamura, K., and Stocker, T. F.: High-resolution carbon dioxide concentration record 650,000-800,000 years before present, Nature, 453, 379–382, doi:10.1038/nature06949, 2008.
Marin, F. and Luquet, G.: Molluscan shell proteins, C. R. Palevol, 3, 469–492, 2004.
Michaelidis, B., Ouzounis, C., Paleras, A., and Portner, H. O.: Effects of long-term moderate hypercapnia on acid-base balance and growth rate in marine mussels *Mytilus galloprovincialis*, Mar. Ecol.-Prog. Ser., 293, 109–118, 2005.
Mutterlose, J., Linnert, C., and Norris, R.: Calcareous nannofossils from the Paleocene-Eocene Thermal Maximum of the equatorial Atlantic (ODP site 1260b): Evidence for tropical warming, Mar. Micropaleontol., 65, 13–31, doi:10.1016/j.marmicro.2007.05.0047, 2007.
Orr, J. C., Fabry, V. J., Aumont, O., Bopp, L., Doney, S. C., Feely, R. A., Gnanadesikan, A., Gruber, N., Ishida, A., Joos, F., Key, R. M., Lindsay, K., Maier-Reimer, E., Matear, R., Monfray, P., Mouchet, A., Najjar, R. G., Plattner, G. K., Rodgers, K. B., Sabine, C. L., Sarmiento, J. L., Schlitzer, R., Slater, R. D., Totterdell, I. J., Weirig, M. F., Yamanaka, Y., and Yool, A.: Anthropogenic ocean acidification over the twenty-first century and its impact on calcifying organisms, Nature, 437, 681–686, doi:10.1038/nature04095, 2005.
Pancost, R. D., Steart, D. S., Handley, L., Collinson, M. E., Hooker, J. J., Scott, A. C., Grassineau, N. V., and Glasspool, I. J.: Increased terrestrial methane cycling at the Palaeocene-Eocene Thermal Maximum, Nature, 449, 332–336, doi:10.1038/nature06012, 2007.
Pierre, C.: The oxygen and carbon isotope distribution in the Mediterranean water masses, Mar. Geol., 153, 41–55, doi:10.1016/s0025-3227(98)00090-5, 1999.
Pouchou, J. L. and Pichoir, F.: A new model for quantitative x-ray-microanalysis, Part 2, Application to in-depth analysis of heterogeneous samples, Rech. Aerospatiale, 349–367, 1984.
Raffi, I., Backman, J., and Palike, H.: Changes in calcareous nannofossil assemblages across the Paleocene/Eocene transition from the paleo-equatorial pacific ocean, Palaeogeogr. Palaeocl., 226, 93–126, doi:10.1016/j.palaeo.2005.05.006, 2005.
Rodolfo-Metalpa, R., Lombardi, C., Cocito, S., Hall-Spencer, J., and Gambi, M. C.: Effects of ocean acidification and high temperatures on the bryozoan *Myriapora truncata* and natural CO_2 vents, Mar. Ecol., 1–10, doi:10.1111/j.1439-0485.2009.00354.x, 2010.
Rodolfo-Metalpa, R., Houlbrèque, F., Tambutté, E., Boisson, F., Baggini, C., Patti, F. P., Jeffree,

R., Fine, M., Foggo, A., Gattuso, J.-P., and Hall-Spencer, J. M.: Coral and mollusc resistance to ocean acidification adversely affected by warming, Nature Climate Change Letters, 1, 308–312 doi:10.1038/NCLIMATE1200, 2011.

Scheibner, C. and Speijer, R. P.: Late Paleocene-Early Eocene Tethyan carbonate platform evolution – a response to long- and short-term paleoclimatic change, Earth-Sci. Rev., 90, 71–102, doi:10.1016/j.earscirev.2008.07.002, 2008.

Shumway, S. E.: Effect of salinity fluctuation on osmotic-pressure and Na^{+}, Ca^{2+} and Mg^{2+} ion concentrations in hemolymph of bivalve mollusks, Mar. Biol., 41, 153–177, 1977.

Sluijs, A. , Brinkhuis, H., Schouten, S., Bohaty, S. M., John, C. M., Zachos, J. C., Reichart, G. J., Damste, J. S. S., Crouch, E. M., and Dickens, G. R.: Environmental precursors to rapid light carbon injection at the Palaeocene/Eocene boundary, Nature, 450, 1218–1215, doi:10.1038/nature06400, 2007.

Solomon, S., Plattner, G. K., Knutti, R., and Friedlingstein, P.: Irreversible climate change due to carbon dioxide emissions, P. Natl. Acad. Sci. USA, 106, 1704–1709, doi:10.1073/pnas.0812721106, 2009.

Thomsen, J. and Melzner, F.: Moderate seawater acidification does not elicit long-term metabolic depression in the blue mussel *Mytilus edulis*, Mar. Biol., 157, 2667–2676, doi:10.1007/s00227-010-1527-0, 2010.

Thomsen, J., Gutowska, M. A., Saphörster, J., Heinemann, A., Trübenbach, K., Fietzke, J., Hiebenthal, C., Eisenhauer, A., Körtzinger, A., Wahl, M., and Melzner, F.: Calcifying invertebrates succeed in a naturally CO_2 enriched coastal habitat but are threatened by high levels of future acidification, Biogeosciences Discuss., 7, 5119–5156, doi:10.5194/bgd-7-5119-2010, 2010.

Tynan, S., Opkyke, B. N., Ellis, D., and Beavis, S.: A history of heavy metal pollution recorded in the shell of *Mytilus edulis*, Geochim. Cosmochim. Acta, 70, A662–A662, doi:10.1016/j.gca.2006.06.1235, 2006.

Vander Putten, E., Dehairs, F., Keppens, E., and Baeyens, W.: High resolution distribution of trace elements in the calcite shell layer of modern *Mytilus edulis*: Environmental and biological controls, Geochim. Cosmochim. Acta, 64, 997–1011, 2000.

Wanamaker, A. D., Kreutz, K. J., Borns, H. W., Introne, D. S., Feindel, S., Funder, S., Rawson, P. D., and Barber, B. J.: Experimental determination of salinity, temperature, growth, and metabolic effects on shell isotope chemistry of *Mytilus edulis* collected from Maine and Greenland, Paleoceanography, 22, 1–12, doi:10.1029/2006pa001352, 2007.

Watabe, N., Kingsley, R. J., and Crick, R. E.: Extra-, inter-, and intracellular mineralization in invertebrates and algae, Origin, evolution and modern aspects of biomineralization in plants and animals, 209–223, Plenum Press, NY, 1990.

Weiner, S. and Dove, P. M.: An overview of biomineralization processes and the problem of the vital effect, Biomineralization, 54, 1–29, 2003.

Westerhold, T., Rohl, U., Laskar, J., Raffi, I., Bowles, J., Lourens, L. J., and Zachos, J. C.: On the duration of magnetochrons C24r and C25n and the timing of early Eocene global warming events: Implications from the ocean drilling program leg 208 walvis ridge depth transect, Paleoceanography, 22, 1–19, doi:10.1029/2006pa001322, 2007.

Witbaard, R., Jenness, M. I., Vanderborg, K., and Ganssen, G.: Verification of annual growth increments in *Arctica islandica* Part I, From the North Sea by means of oxygen and carbon isotopes, Neth. J. Sea Res., 33, 91–101, 1994.

Zachos, J. C., Rohl, U., Schellenberg, S. A., Sluijs, A., Hodell, D. A., Kelly, D. C., Thomas, E., Nicolo, M., Raffi, I., Lourens, L. J., McCarren, H., and Kroon, D.: Rapid acidification of the ocean during the Paleocene-Eocene Thermal Maximum, Science, 308, 1611–1615, doi:10.1126/science.1109004, 2005.

Table 1. Parameters of field experimental sites. Mean ± S.D. seawater chemistry calculated over the experiment period at the two experiment sites B1 and C. pH_T is in total scale; pCO_2 in µatm; HCO_3^-, CO_3^{2-}, CO_2 and DIC (dissolved inorganic carbon) are in µmol kg^{-1}; saturation state (Ω) of aragonite and calcite. Seawater isotope data are from Pierre (1999). Note, seawater parameters in the harbour of Ischia are nearly identical to those of site C.

	T (°C)	pH_T	pCO_2 (µatm)	HCO_3^- (µmol kg^{-1})	CO_3^{2-} (µmol kg^{-1})	CO_2 (µmol kg^{-1})	DIC (µmol kg^{-1})	Ω calcite	Ω aragonite	$\delta^{18}O$ (‰)	$\delta^{13}C$ (‰)
Site C	21.0 (±4.2)	8.07 (±0.04)	474 (±58)	2015 (±74)	235 (±35)	15 (±2)	2265 (±43)	5.42 (±0.74)	3.55 (±0.52)	1.2–1.3 (±0.02)	1.4 (±0.02)
Site B1	20.7 (±4.2)	7.25 (±0.44)	5494 (±5520)	2428 (±108)	61 (±45)	173 (±175)	2661 (±226)	1.37 (±0.95)	0.98 (±0.69)	1.2–1.3 (±0.02)	1.4 (±0.02)

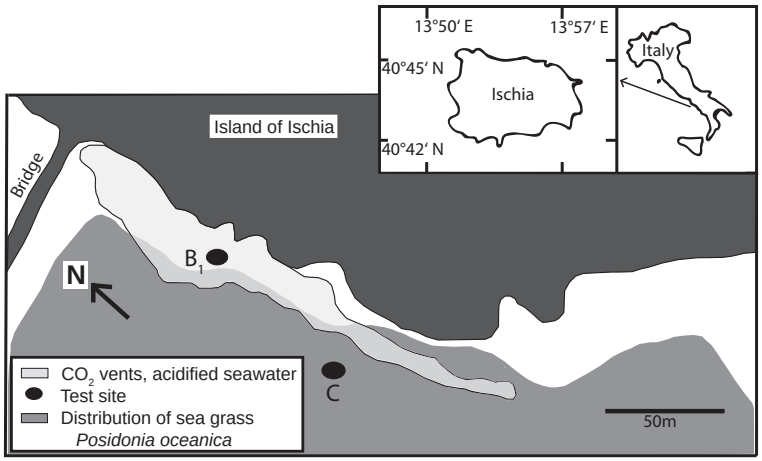

Fig. 1. Schematic map of natural experiment sites off Ischia in the vicinity of CO_2 vents. Specimens of *M. galloprovincialis* were transplanted to experimental sites C (mean pH_T 8.07) and B1 (mean pH_T of 7.25, minimum pH_T 6.83). Site C was used as a control locality (map modified after Hall-Spencer et al., 2008).

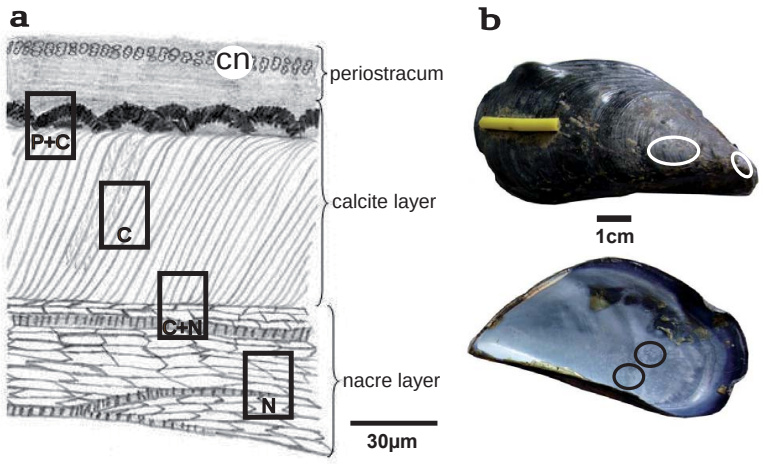

Fig. 2. **(a)** Sketch of tripartite shell structure of *M. galloprovincialis*. Note periostracum, calcite and aragonitic nacre layers. Black boxes indicates sampling sites for isotope analysis. P + C = periostracum and calcite layer; C = calcite layer; C + N = calcite and nacre layer; N = nacre layer. "Cn" indicates channel network ("pipe system") in the upper part of the periostracum. **(b)** *Mytilus galloprovincialis* from site B1. Note partial lack of periostracum (white circles) and absence of encrusting or colonizing marine biota in upper image and incomplete nacre layer (black circles) in lower image. On 26 September 2009, i.e. prior to transplantation, specimens were labelled with a yellow marker in order to differentiate pre- and post-transplantation shell material.

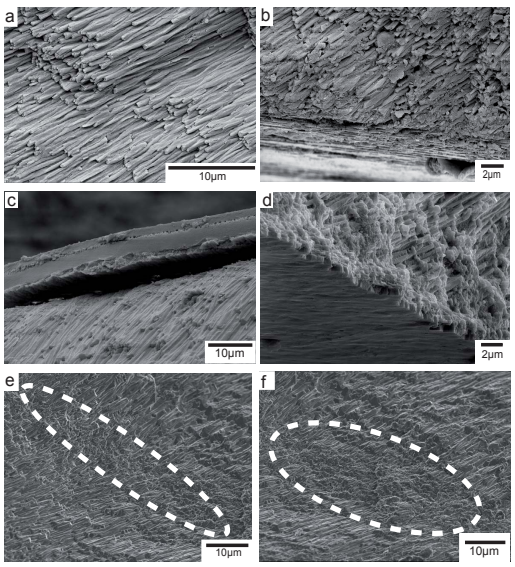

Fig. 3. Calcite layer SEM images from three different *Mytilidae*. Images are from outer margin precipitated from normal marine seawater pH **(a–d)** and from shells precipitated from acidified seawater **(e, f)**. **(a, b)** Calcite layer of reference specimen of *M. edulis* from Sylt characterized by well structured calcite layer. **(c, d)** Calcite layer of *M. galloprovincialis* from experimental site C (pH_T = 8.07). Note well structured calcite layer similar to **(a)** and **(b)**. **(e, f)** Calcite layer of *M. galloprovincialis* from acidified experimental site B1. Note portions of calcite layer with disorganized shell structure (white stippled line) within otherwise organized calcite shell.

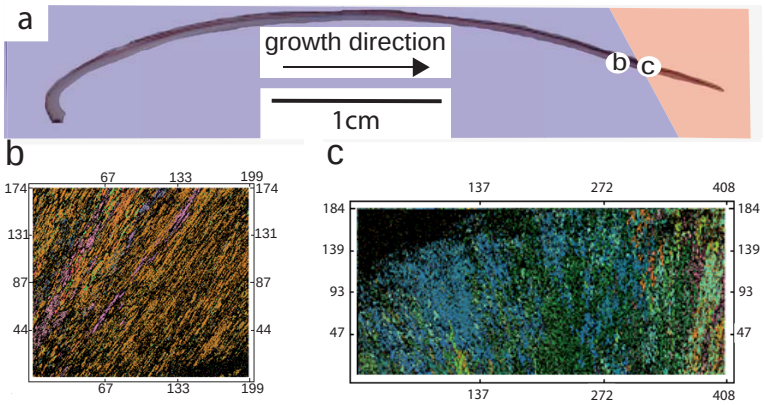

Fig. 4. Thin-section view of *M. galloprovincialis* from site B1. **(a)** Blue colour indicates shell precipitated prior to transplantation and red colour indicates shell precipitated after transplantation to acidified test site. **(b, c)** Electron backscatter diffraction (EBSD) maps. Note location of b and c in **(a)**. Different colours indicate different orientations of calcite fibres. Note rather homogenous (brown to yellow, **(b)** colours in well structure calcite shell prior to transplantation. The EBSD map of shell portions precipitated after the transplantation indicates a wider range of colours and spatially disorganized calcite fibres indicating shell precipitation under acidified environments.

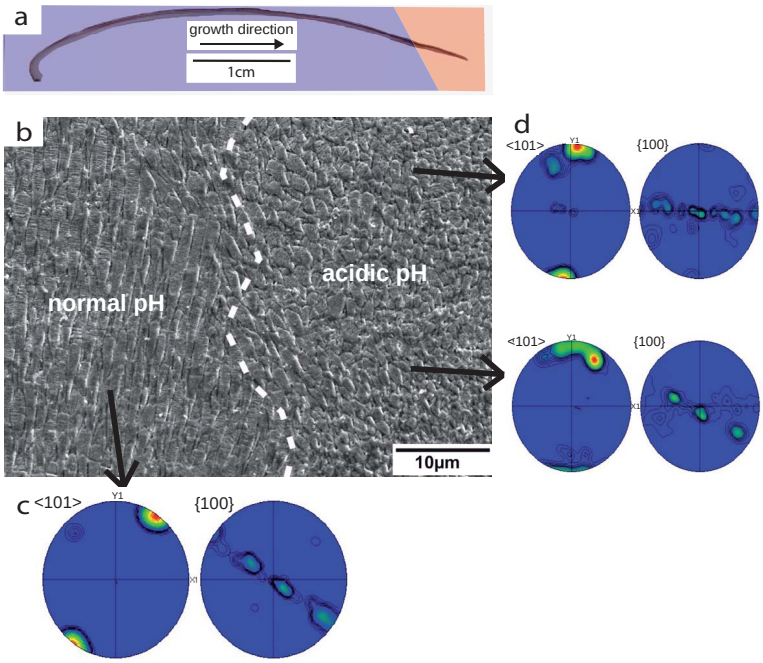

Fig. 5. Thin section view of calcite layer of *M. galloprovincialis* from acidified seawater site B1. **(a)** Blue colour indicates shell precipitated prior to transplantation and red colour indicates shell precipitated after transplantation to acidified test site B1. **(b)** SEM image of shell precipitated directly before and after transplantation. Note pronounced differences in the orientation of the calcite layer across transplantation event (white, stippled line). Locations of respective pole figures c and d are indicated. **(c, d)** Pole figures representing stereographic projections of crystallographic axes and planes.

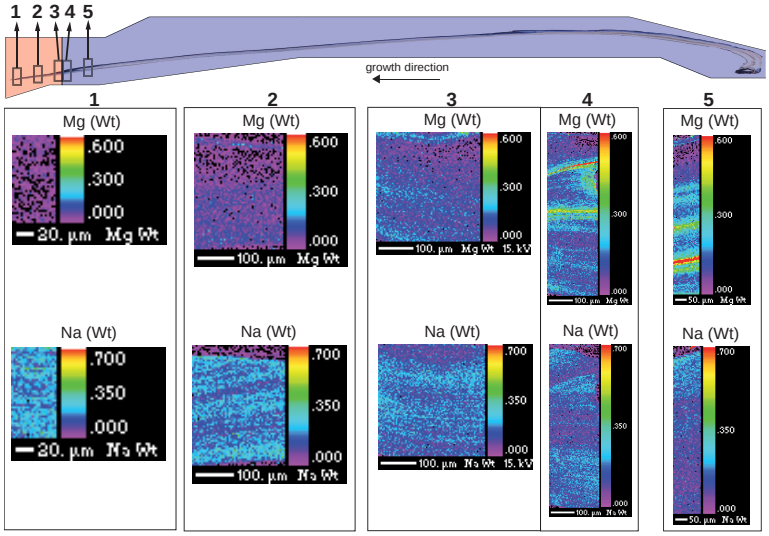

Fig. 6. Thin section view of *M. galloprovincialis* from acidified seawater site B1. Blue colour indicates shell precipitated prior to transplantation and red colour indicates shell precipitated after transplantation to acidified test site. Gray boxes numbered 1 through 5 indicate the position of the microprobe maps. Magnesium and sodium microprobe maps 1 through 5 are numbered in ascending order from the commissure to the hinge (corresponding to the boxes with the microprobe maps). Due to the incisive difference between the element Magnesium (Mg) and Sodium (Na), these elements are illustrated. The concentration of elements is given in weight percent (Wt). The element distribution in the shell displays no discernible patter while concentrations of Mg and Na follow opposite trends.

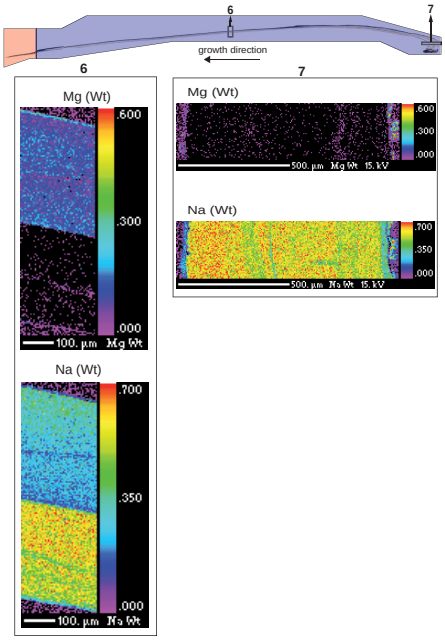

Fig. 7. Thin section view of *M. galloprovincialis* from acidified seawater site B1. Blue colour indicates shell precipitated prior to transplantation and red colour indicates shell precipitated after transplantation to acidified test site. Gray boxes numbered 6 and 7 from mid-shell and hinge indicate the position of the microprobe maps. Magnesium and sodium concentration is given in weight percent. Differences in element concentrations in map 6 reflect differences between calcite and aragonite layer. Magnesium and sodium are incorporated in calcite layer. Nacre layer displays considerably higher concentrations of sodium. Judging from elemental maps, the shell hinge is composed almost entirely of aragonite.

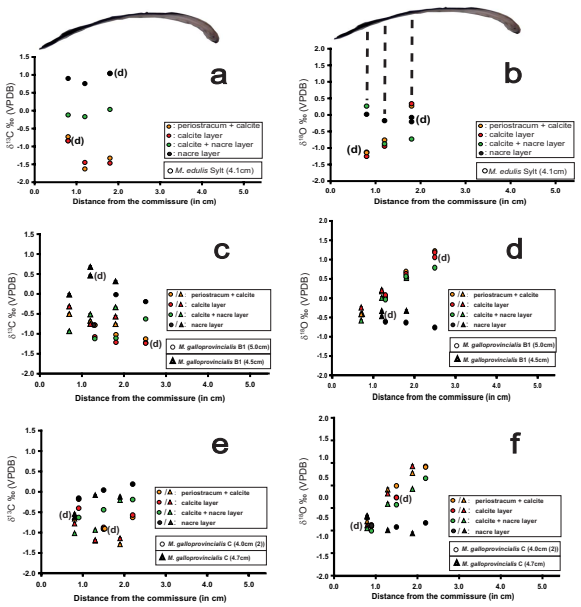

Fig. 8. Differential carbon and oxygen isotope ratios representing shell layer and bulk samples of one specimen of *M. edulis* **(a, b)** and four specimens of *M. galloprovincialis* $_{B1 \text{ and } C}$ **(c–f)** plotted against distance from commissure. Different specimen are characterized by their different shell length and experimental site, e.g. *M. galloprovincialis* C (4.0 cm) refers to a specimen with a shell length of 4 cm that was dislocated to experimental site C. **(a, b)** *Mytilus edulis* isotope data for reference. This specimen is from normal seawater pH (Wadden Sea) and has not been dislocated. **(c–f)** *Mytilus galloprovincialis* shell isotope values from experimental sites B1 **(c, d)** and C **(e, f)**. Colour code represents different layers analyzed. Note considerable differences in isotope values from different shell layers.

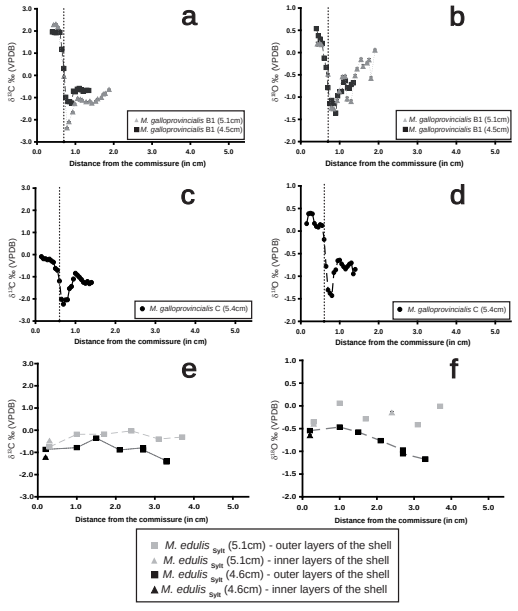

Fig. 9. Times series $\delta^{13}C$ and $\delta^{18}O$ ratios plotted against distance from shell commissure. Different specimens/shells are labelled according to shell length. *Mytilus edulis*$_{Sylt}$ (4.6 cm) refers, for example, to a specimen with shell length of 4.6 cm from the Sylt site (List, Wadden Sea Station). **(a, b)** Data from *M. galloprovincialis* $_{B1}$ showing transition from Ischia harbour to acidified experimental site. Data plotted to the left of horizontal, black stippled line indicate analytical data from shell material precipitated after transplantation. Note considerable negative excursion in both carbon and oxygen data followed by marked positive trend. Negative $\delta^{18}O$ shift is probably best interpreted as effect of an anomalous warm and long heat-wave, which affected the marine life in summer 2009. Positive shift cannot be related to temperature alone and is probably related to seawater pH change and metabolic effects. **(c, d)** Data from *M. galloprovincialis* $_{C}$ showing transition from Ischia harbour to normal pH experimental site. Near identical isotope pattern as recorded at site B1 is found albeit with smaller amplitudes. **(e, f)** Data from *M. edulis*$_{Sylt}$ reference shells precipitated without transplantation bias from normal pH conditions. Moderate shifts in carbon are explained in the context of food availability whilst oxygen reflects trends in mainly seawater temperature.